



## An adaptive finite element procedure for crack propagation analysis

ALSHOAIBI Abdunaser M.<sup>†</sup>, HADI M.S.A., ARIFFIN A.K.

(Department of Mechanical & Materials Engineering, Universiti Kebangsaan Malaysia, 43600 Bangi, Selangor Darul Ehsan, Malaysia)

<sup>†</sup>E-mail: alshoaibi@gmail.com; alhager01@yahoo.com

Received May 14, 2006; revision accepted Oct. 10, 2006

**Abstract:** This paper presents the adaptive mesh finite element estimation method for analyzing 2D linear elastic fracture problems. The mesh is generated by the advancing front method and the norm stress error is taken as a posteriori error estimator for the h-type adaptive refinement. The stress intensity factors are estimated by a displacement extrapolation technique. The near crack tip displacements used are obtained from specific nodes of natural six-noded quarter-point elements which are generated around the crack tip defined by the user. The crack growth and its direction are determined by the calculated stress intensity factors. The maximum circumference theory is used for the latter. In evaluating the accuracy of the estimated stress intensity factors, four cases are tested consisting of compact tension specimen, three-point bending specimen, central cracked plate and double edge notched plate. These were carried out and compared to the results from other studies. The crack trajectories of these specimen tests are also illustrated.

**Key words:** Linear elastic fracture mechanics, Adaptive refinement, Stress intensity factors, Crack propagation

**doi:** 10.1631/jzus.2007.A0228

**Document code:** A

**CLC number:** O346.1; TB303

### INTRODUCTION

The finite element method (FEM) has proved to be very well suited for the study of fracture mechanics. Nevertheless, modelling the propagation of a crack through a finite element mesh turns out to be difficult because of the modification of the mesh topology. Use of crack propagation laws based on stress intensity factor range is the most successful engineering application of fracture mechanics. The stress intensity factors are a very important parameter in fracture analysis. These factors define the stress field close to the crack tip of a crack and provide fundamental information on how the crack is going to propagate. In linear elastic fracture problem, the prediction of the crack growth and the crack direction are determined by the stress intensity factor. Several methods have been proposed to numerically estimate stress intensity factors using FEM such as the displacement extrapolation technique, the  $J$ -integral and the energy domain integral. The first method is used when the singular elements are present at the crack tip. In the finite element fracture analysis, these special ele-

ments known as quarter-point elements are used to provide the element polynomial representing the stresses and strains field singularity near the crack tip. Nodal relaxation is used to release nodes, one by one, in order to enable the crack tip to propagate through the mesh. This method which is based on near-tip field fitting procedures requires finer meshes to produce a good numerical representation of crack-tip fields with the most accurate methods being those based on nodal displacements, which are a primary output of the finite element program (Guinea *et al.*, 2000). In adaptive mesh refinement, most analysts favour either the Delaunay technique or the advancing front method over other techniques when generating meshes due to the quality of unstructured meshes generated (El-Hamalawi, 2004). The main advantage of the advancing front method is that it tends to produce nicely graded meshes and high quality triangles that are usually very close in shape to equilaterals. The boundary integrity is also preserved, since the discretisation of the domain boundary constitutes the initial front. This is in contrast to the Delaunay triangulation, where boundary integrity is not

usually preserved for complicated domains, which is a key requirement for mesh generation procedures (El-Hamalawi, 2004).

The main objective of this paper is to determine the stress intensity factor for crack propagation problem under linear elastic fracture analysis using the displacement extrapolation technique with adaptive FEM. The computational code is written in FORTRAN. The mesh for finite elements is the unstructured type, generated using the advancing front method. The global h-type adaptive mesh is adopted based on the norm stress error estimator. The quarter-point singular elements are uniformly generated around the crack tip in the form of a rosette. The displacement extrapolation technique used in the calculation is explained. The algorithm is assessed by considering four standard test specimen geometries, i.e. compact tension specimen, three-point bending specimen, double edge notched plate, central cracked plate, and single edge cracked plate.

#### ADAPTIVE MESH GENERATION AND REFINEMENT

In this work, the unstructured triangle mesh is automatically generated by employing the advancing front method (Löhner, 1997). This technique however requires generating background mesh in order to accurately control the distribution of the geometrical characteristics such as the element size, element stretching and stretching directions for the new mesh. The background does not have to be precisely representing the geometry; however the accuracy of the distribution depends on this excellence and it must completely cover the computational domain (Zienkiewicz *et al.*, 2005). Here the strategy taken to generate the background mesh is to utilize all the initial boundary nodes of geometry and construct the boundary triangles as the background mesh by the dichotomy technique. In this technique the computational domain must be a polygon since the boundary triangulations are carried out by means of dividing and repeatedly dividing the polygon into two subsets until the simplest polygon subsets i.e. the boundary triangles, are yielded. Therefore, if there are any internal boundaries representing for example holes, then connector lines must be introduced connecting

each internal boundary to the external boundary. This will force the internal boundaries to be part of a continuous line of the externals and therefore set the computational domain to be a polygon. In order to do this, the orientation direction of internal boundaries is set clockwise while for external boundary is set the other way round. The connector line is introduced by finding the nearest distance between any internal boundary points to any of the external ones (Sezer and Zeid, 1991).

In the proposed dichotomy method, the division starts at any first found boundary point with large face angle and setting an angle range for searching the nearest nonadjacent point to be connected by a division line. The angle range is set in such a way that the division can produce high quality polygon subset shape. If the search for the nearest nonadjacent point failed, then the division can be initiated at a boundary point with smaller face angle. The classification order of the face angle size  $\theta_i$  is set as  $\pi \leq \theta_1 < 2\pi$ ,  $\pi/2 < \theta_2 < \pi$ ,  $0 < \theta_3 \leq \pi/2$ .

In order to properly represent the field singularity around the crack tip, the singular elements have to be constructed as well. Since the advancing front method generates the triangle elements starting from the boundary faces, the area around the crack tip for the construction of the singular elements is supposed to be isolated. This area is isolated by first generating nodes around the crack tip in the rosette form and then the crack tip node and the jointed boundary segments are removed. New boundary segments are then introduced linking all the new nodes to temporarily 'cut out' the template area from the original domain. Subsequently the advancing front triangulation can be executed. Finally singular elements are 'patched' into the rosette template to complete the process. This procedure is illustrated by Fig.1. The numbers of elements depend on the distributed nodes around the crack tip, which can be set by user.

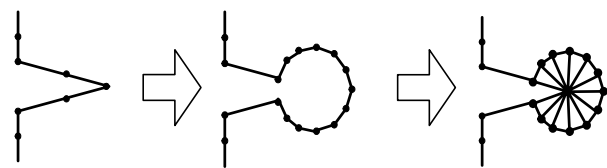


**Fig.1 The cut and patch procedure of generating singular elements around a crack tip**

Fig.2 shows example geometry where the whole process of generating the mesh is illustrated for better understanding. Fig.2a illustrates the geometry of a plate with six holes and two notches. Fig.2b shows six connector lines forcing the internal boundaries to be the continuous part of the external boundary. Fig.2c shows the cutting out of the rosette templates around each crack tip. The background mesh for this domain is then set up automatically using dichotomy technique as shown in Fig.2d. Fig.2e shows the conventional mesh being generated by the advancing front method. The first generation produces mesh with initial size set by user. Later, during adaptive refinement, this first generated mesh will be taken as the background mesh. In Fig.2f, for each rosette template, quarter-point elements are then constructed. Fig.2g shows the enlargement of the quarter-point element at one of the crack tip.

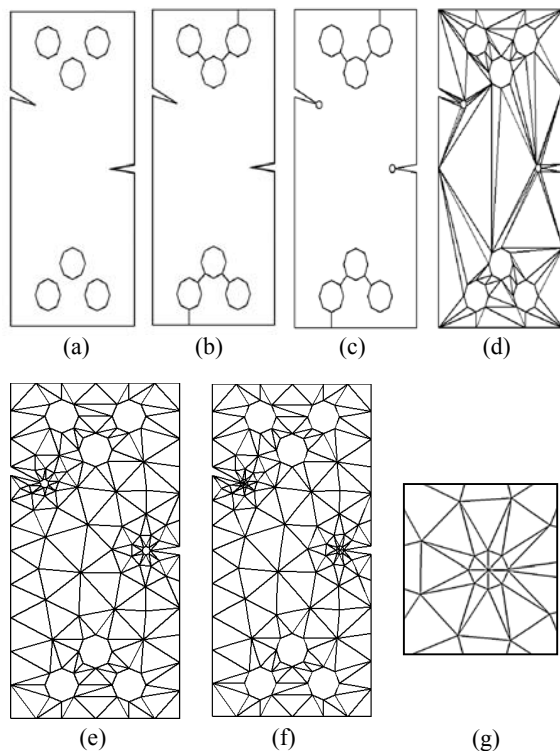


Fig.2 (a)-(g) showing the mesh generation stages with inclusion of quarter point elements

In general, smaller mesh size gives more accurate finite element approximate solution. However, reduction in the mesh size leads to greater computational effort.

The adaptive mesh refinement is based on a posteriori error estimator which is obtained from the solution from the previous mesh. The error estimator used in this paper is based on stress error norm. The strategy used to refine the mesh during analysis process is adopted from (Ariffin, 1995) as follows:

- (1) Determine the error norm for each element

$$\|E\|_e = \int_{\Omega_e} (\boldsymbol{\sigma} - \boldsymbol{\sigma}^*)^T (\boldsymbol{\sigma} - \boldsymbol{\sigma}^*) d\Omega, \quad (1)$$

where  $E$  is the error estimator,  $e$  is the current element,  $\Omega_e$  is the area of the current element,  $\boldsymbol{\sigma}$  is the stress field obtained from the finite element calculation and  $\boldsymbol{\sigma}^*$  is the smoothed stress field.

- (2) Determine the average error norm over the whole domain

$$\|\hat{E}\| = \frac{1}{m} \sum_{e=1}^m \int_{\Omega_e} \boldsymbol{\sigma}^T \boldsymbol{\sigma} d\Omega, \quad (2)$$

where  $m$  is the total number of elements in the whole domain.

- (3) Determine a variable  $\varepsilon_e$  for each element as

$$\varepsilon_e = \frac{1}{\eta} \frac{(\|E\|_e)^{1/2}}{(\|\hat{E}\|)^{1/2}}, \quad (3)$$

where  $\eta$  is a percentage that measures the permissible error for each element. If  $\varepsilon_e > 1$  the size of the element is reduced and vice versa.

- (4) The new element size is determined as

$$\hat{h}_e = h_e / (\varepsilon_e)^{1/p}, \quad (4)$$

where  $h_e$  is the old element size and  $p$  is the order of the interpolation shape function.

## STRESS INTENSITY FACTOR AND CRACK PROPAGATION

In this paper, the displacement extrapolation method (Phongthanapanich and Dechaumphai, 2004) is used to calculate the stress intensity factors as follows:

$$K_I = \frac{E}{3(1+\nu)(1+\kappa)} \sqrt{\frac{2\pi}{L}} \left[ 4(v'_b - v'_d) - \frac{(v'_c - v'_e)}{2} \right], \quad (5)$$

$$K_{II} = \frac{E}{3(1+\nu)(1+\kappa)} \sqrt{\frac{2\pi}{L}} \left[ 4(u'_b - u'_d) - \frac{(u'_c - u'_e)}{2} \right], \quad (6)$$

where  $E$  is the modulus of elasticity,  $\nu$  is the Poisson's ratio,  $\kappa$  is the elastic parameter defined by

$$\kappa = \begin{cases} (3 - 4\nu) & \text{plane stress,} \\ (3 - 4\nu)/(1 + \nu) & \text{plane strain,} \end{cases}$$

and  $L$  is the quarter-point element length. The  $u'$  and  $v'$  are the displacement components in the  $x'$  and  $y'$  directions, respectively; the subscripts indicate their position as shown in Fig.3.

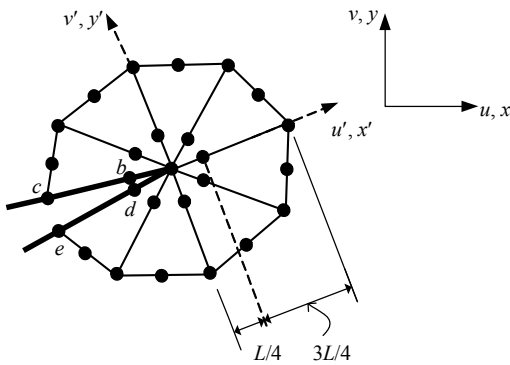


Fig.3 The arrangement of the natural quarter-point triangular elements around the crack tip

In order to simulate crack propagation under linear elastic condition, the crack path direction must be determined.

There are several methods used to predict the direction of crack trajectory such as the maximum circumferential stress theory, the maximum energy release rate theory and the minimum strain energy density theory.

The maximum circumferential stress theory states that, for isotropic materials under mixed-mode loading, the crack will propagate in a direction normal to maximum tangential tensile stress. In polar coordinates, the tangential stress is given by

$$\sigma_\theta = \frac{1}{\sqrt{2\pi r}} \cos \frac{\theta}{2} \left[ K_I \cos^2 \frac{\theta}{2} - \frac{3}{2} K_{II} \sin \theta \right]. \quad (7)$$

The direction normal to the maximum tangential stress can be obtained by solving  $d\sigma_\theta/d\theta=0$  for  $\theta$ . The nontrivial solution is given by

$$K_I \sin \theta + K_{II} (3 \cos \theta - 1) = 0, \quad (8)$$

which can be solved as:

$$\theta_0 = \pm \cos^{-1} \left\{ \frac{3K_{II}^2 + K_I \sqrt{K_I^2 + 8K_{II}^2}}{K_I^2 + 9K_{II}^2} \right\} \quad (9)$$

In order to ensure that the opening stress associated with the crack direction of the crack extension is maximum, the sign of  $\theta_0$  should be opposite to the sign of  $K_{II}$  (Andersen, 1998).

The criterion for crack to propagate from crack tip is based on the material toughness  $K_c$ . If the calculated stress intensity factor,  $K_I \geq K_c$  then the crack will propagate in the direction  $\theta_0$  expressed by Eq.(9). The crack increment length  $\Delta a$  is taken as 10%~20% of the initial crack length  $a$ , inversely proportional to the ratio of  $K_{II}/K_I$ . The ratio represents the mixed mode proportionality, therefore shorter increment length should be taken to carefully justify the crack path curvature when  $K_{II}$  is relatively large compared to  $K_I$  (Bittencourt et al., 1996).

## NUMERICAL ANALYSIS AND RESULTS

In order to carry comprehensively evaluate the stress intensity factors approximated by the developed program, four well-known plate geometries, compact tension specimen, three-points bending specimen, central cracked plate and double edge notched plate are considered.

### Compact tension specimen

The compact tension test specimen geometry and the final adaptive mesh are shown in Fig.4. The specimen has an initial crack length  $a=9$  cm, width  $W=18.8$  cm, and the thickness  $B$ , has various values as explained below.

The analytical stress intensity factor for this geometry can be calculated from (Anderson, 1994) as follows:

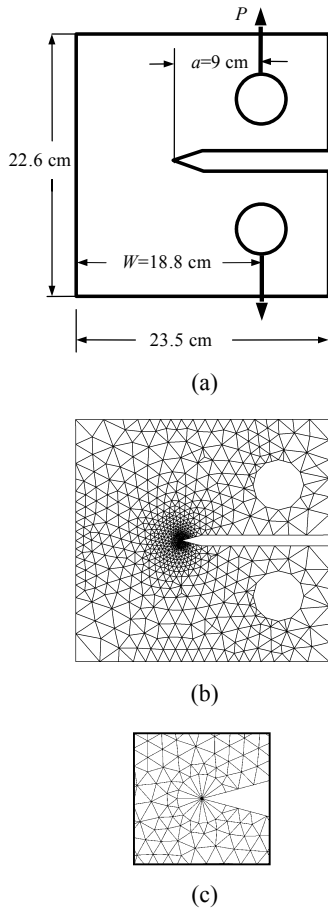


Fig.4 Compact tension geometry (a), the final adaptive mesh (b) and the zooming of mesh (c) around crack tip

$$K_I = P \left( 2 + \frac{a}{W} \right) \left[ 0.886 + 4.64 \left( \frac{a}{W} \right) - 13.32 \left( \frac{a}{W} \right)^2 + 14.72 \left( \frac{a}{W} \right)^3 - 5.6 \left( \frac{a}{W} \right)^4 \right] / \left[ B \sqrt{W} \left( 1 - \frac{a}{W} \right)^{3/2} \right], \quad (10)$$

where  $P$  is the applied load.

The computed values of the stress intensity factor under plane stress condition are compared with the experimental and numerical results obtained from (Parnas *et al.*, 1996) as shown in Fig.5. In their study, steel plates, with modulus of elasticity 210 GPa and Poisson's ratio of 0.3, are used. Steel specimens with thickness of 8.3 and 13.6 mm are considered. The experimental results are compared with finite element results using ANSYS software (Fig.5a). The comparison also comprises the analytical solution (Fig.5). The results of the steel specimens show obviously the effect of the variation of the two thicknesses on

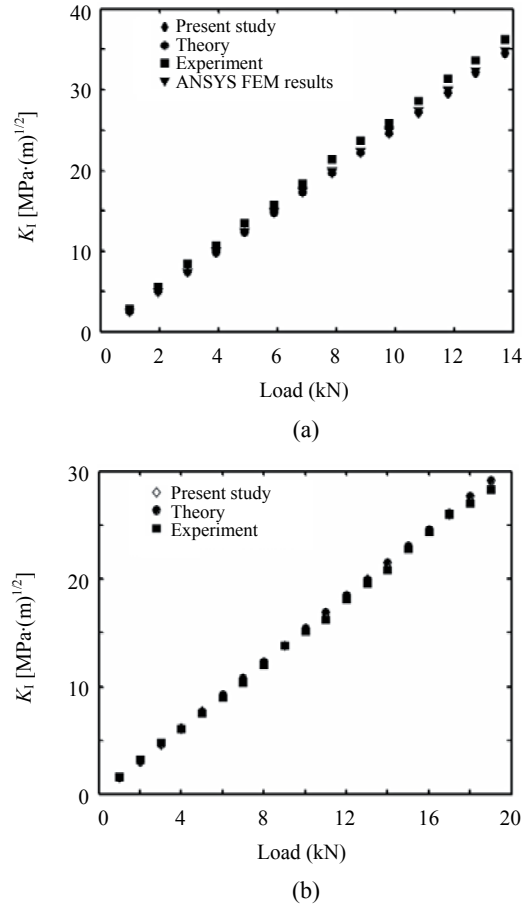


Fig.5 Stress intensity factor values for steel specimen. (a)  $h=8.3$  mm; (b)  $h=13.6$  mm

the stress intensity factors results.

The present values of stress intensity factors are very close to the theoretical solutions and are in good agreement with the experimental results.

Fig.6 shows four steps of crack propagation. The predicted crack propagation seems to follow the mode I trajectory very well.

### Three-point bend specimen

The geometry of the three-point bend specimen and the final adaptive mesh are shown in Fig.7. The analytical stress intensity factor for this problem can be calculated from (Broek, 1986) as:

$$K_I = \frac{PS}{BW^{3/2}} \left[ 2.9 \left( \frac{a}{W} \right)^{1/2} - 4.6 \left( \frac{a}{W} \right)^{3/2} + 21.8 \left( \frac{a}{W} \right)^{5/2} - 37.6 \left( \frac{a}{W} \right)^{7/2} + 38.7 \left( \frac{a}{W} \right)^{9/2} \right]. \quad (11)$$

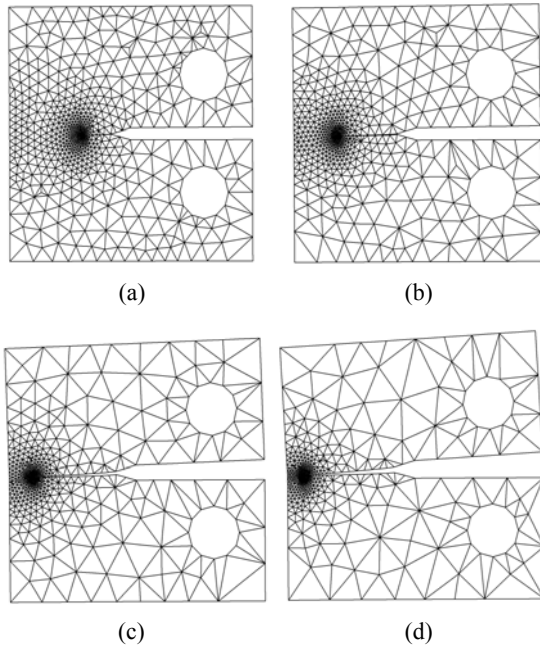


Fig.6 (a)~(d) showing the crack propagation trajectory for a compact tension specimen under Mode I loading

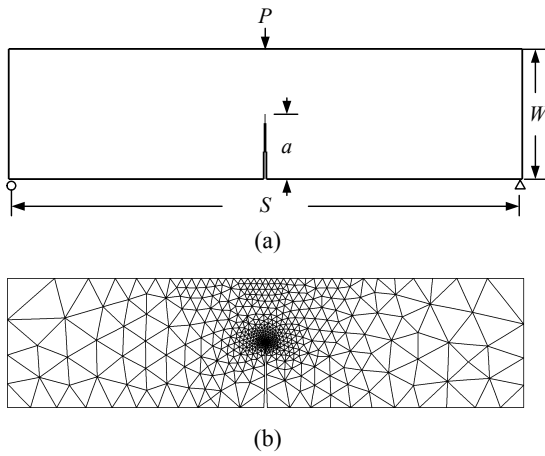


Fig.7 Three-point bend specimen (a) and the final adaptive mesh (b)

The geometry is imposed by plane strain condition with point load  $P$ , span length  $S$ , height  $W$ , thickness  $B$  and crack length  $a$ .

The dimensionless stress intensity factor for this specimen is given by (Freese and Baratta, 2006) as:

$$\bar{K}_I = \left(1 - \frac{a}{W}\right)^{3/2} K_I BW / (6P). \quad (12)$$

The comparison of results from this paper and

those obtained from (Freese and Baratta, 2006; Orang, 1988; Fett, 1999) are shown in Table 1 for  $S/W=4$ . The dimensionless form of the estimated stress intensity factor is obtained by Eq.(12). Freese and Baratta (2006) provided values for a range of  $0 < a/W < 1.0$ . Orange (1988) investigated the three-point bend stress intensity factors for short cracks (i.e.  $a/W \leq 0.5$ ) and specifically examined the effect of contact stress due to the center-point load on such factors. Fett (1999) presented for a range of  $0.1 < a/W < 0.8$ . The results in the present study seem to be very close to those of other references.

Table 1 Comparisons of dimensionless stress intensity factors for three-point bend specimen

$a/W$	Dimensionless stress intensity factors			
	Freese and Baratta (2006)	Orange (1988)	Fett (1998)	Present study
0.10	0.832	0.837	0.850	0.82100
0.20	0.700	0.697	0.704	0.69780
0.30	0.612	0.609	0.609	0.60100
0.35	0.576	0.575	–	0.56500
0.40	0.545	0.545	0.545	0.53500
0.45	0.518	0.519	–	0.51010
0.50	0.494	0.494	0.498	0.48936
0.55	0.475	–	–	0.47100
0.60	0.459	–	0.463	0.45260
0.70	0.433	–	0.433	0.43000
0.80	0.410	–	0.408	0.40000
0.90	0.384	–	–	0.38270

Fig.8 shows four steps of crack propagation for the three-point bend specimen. Clearly, the predicted crack opening matches very well the pure Mode I trajectory.

### Central cracked plate

The geometry of the central cracked plat specimen and the final adaptive mesh are shown in Fig.9. The notations for the geometry dimension and crack length are the same as those for the previous specimen and  $\sigma$  is a far field stress.

The analytical stress intensity factor for this problem can be calculated from (Tada et al., 2000) as:

$$K_I = \sigma \sqrt{\pi a} \left[ \sec\left(\frac{\pi a}{2W}\right) \right]^{1/2} \left[ 1 - 0.025 \left(\frac{a}{W}\right)^2 + 0.06 \left(\frac{a}{W}\right)^4 \right]. \quad (13)$$

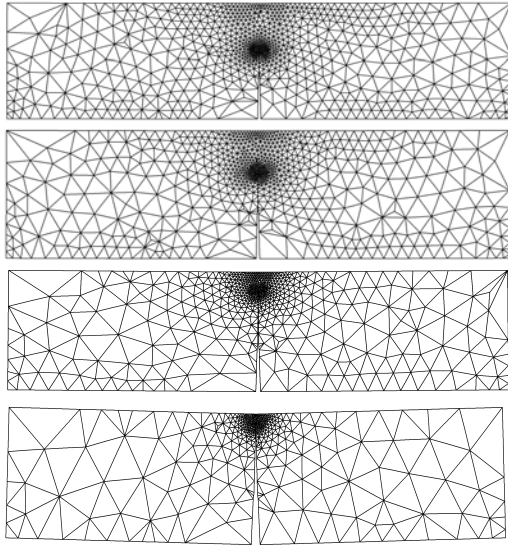


**Fig.8** Adaptive finite element meshes and the crack propagation trajectory for a three-point bend specimen under Mode I loading

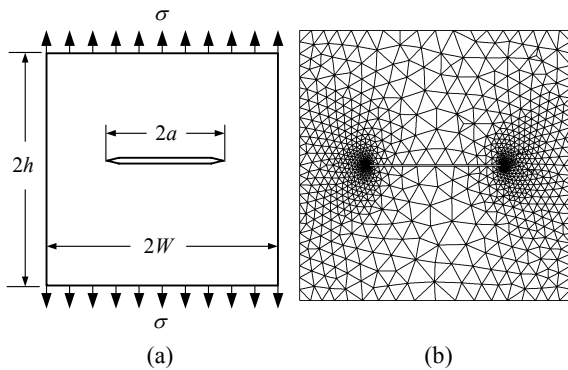


**Fig.9** Central crack plate (a) and the final adaptive mesh (b)

The dimensionless stress intensity factor is given by de Matos *et al.*(2004) as follows:

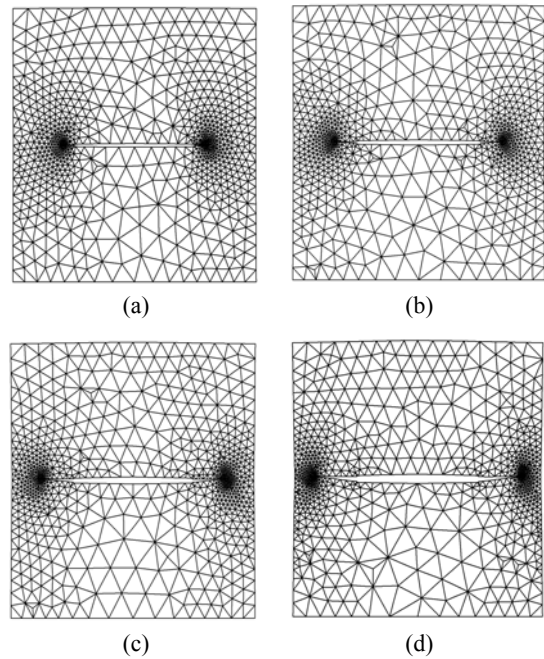
$$\bar{K}_I = K_I / (\sigma\sqrt{\pi a}). \tag{14}$$

Table 2 shows the comparison between the results of stress intensity factors to those from (de Matos *et al.*, 2004) which are estimated using dual boundary element method (DBEM). de Matos *et al.*(2004) also included results of *J*-integral method of Portela (1993) and the analytical solutions of Tada *et al.*(2000). As shown in this table, the agreement is obviously good.

Fig.10 shows four steps of central crack propagation for the initial crack length ratio  $a/W=0.5$ ; the

**Table 2** Non-dimensional stress intensity factor for central crack

$a/W$	$K_I / (\sigma\sqrt{\pi a})$			
	DBEM (Matos <i>et al.</i> , 2004)	<i>J</i> -integral (Portela, 1993)	Tada <i>et al.</i> (2000)	Present study
0.4	1.118	1.114	1.109	1.0900
0.6	1.312	1.308	1.303	1.2747
0.8	1.816	1.815	1.816	1.8131



**Fig.10** (a)~(d) showing the crack propagation trajectory for a central crack plate under mode I loading

predicted crack propagation resembles the experimental results (Simonsen and Tornqvist, 2004).

**Double edge notched plate**

The geometry of the double edge notched plat specimen and the final adaptive mesh are shown in Fig.11.

The analytical stress intensity factor for this problem can be calculated from (Tada *et al.*, 2000) as:

$$K_I = \frac{\sigma\sqrt{\pi a}}{\sqrt{1-\frac{a}{W}}} \left[ 1.122 - 0.561\left(\frac{a}{W}\right) - 0.205\left(\frac{a}{W}\right)^2 + 0.471\left(\frac{a}{W}\right)^3 - 0.190\left(\frac{a}{W}\right)^4 \right]. \tag{15}$$

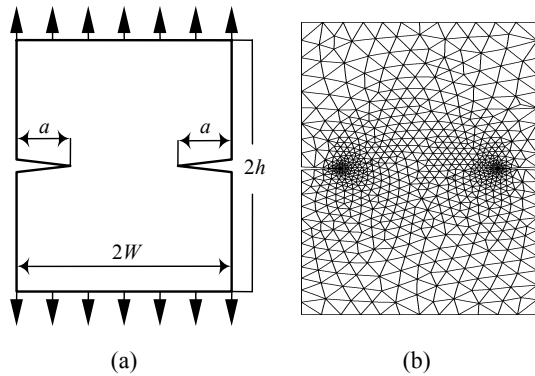


**Fig.11 Double edge notched plate (a) and the final adaptive mesh (b)**

The non-dimensional stress intensity factor can be calculated from (Zhu and Smith, 1995) as follows:

$$\bar{K}_I = K_I / (\sigma \sqrt{\pi a}). \quad (16)$$

The present results for various initial crack lengths shown in Table 3 show close agreement with the analytical solutions calculated by Eq.(15).

**Table 3 Dimensionless stress intensity factor for double edge notched plate**

$a/W$	$K_I / (\sigma \sqrt{\pi a})$	
	Tada <i>et al.</i> (2000)	Present study
0.1	1.1198	1.1166
0.2	1.1215	1.1218
0.3	1.1288	1.1260
0.4	1.1465	1.8930
0.5	1.1812	1.1829
0.6	1.2439	1.2483
0.7	1.3561	1.3560
0.8	1.5727	1.5731
0.9	2.1116	2.1113

Fig.12 shows four steps of central crack propagation for  $a/W=0.5$ . The crack propagates towards the expected path under Mode I loading condition.

**CONCLUSION**

The adaptive finite element method (FEM) using advancing front method for crack propagation analysis and stress intensity factors prediction was

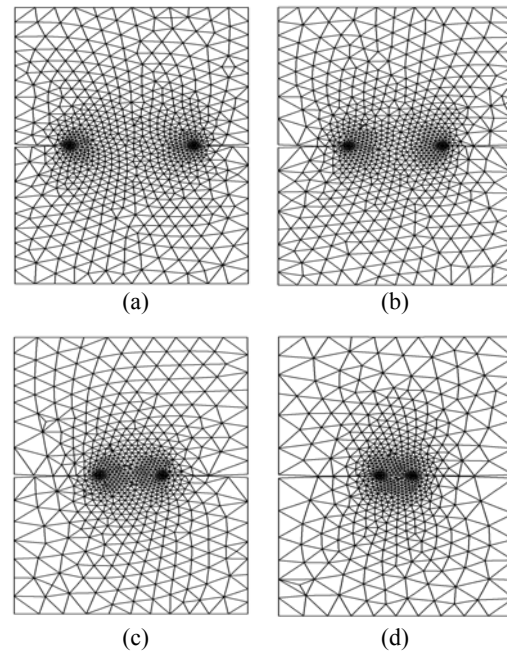


**Fig.12 (a)-(d) showing the crack propagation trajectory for a double edge notched plate under Mode I loading**

presented. The norm stress error is taken as a posterior estimator for the h-type adaptive refinement. The nodes of natural six-node quarter-point elements generated around the crack tip were employed to form a circular zone surrounding the tip in order to better capture the stress field. The adaptive remeshing technique places small elements around the crack tips and in region with large change of stress gradients. At the same time, larger elements are generated in other regions to minimize the total number of unknowns and the computational time. The stress intensity factors are obtained from the extrapolation of displacements at some specific nodes from the quarter-point elements.

The accuracy of the estimated stress intensity factors was evaluated through the assessments comprising four standard plate specimens namely the compact tension specimen, the three-point bending specimen, central cracked plate and double edge notched specimen. The results of stress intensity factors are compared to the closed form solutions and to the extensive results of other researches. The estimated stress intensity factors are used to further approximate the crack increment length and to predict the crack path direction. The prediction of the latter is based on the maximum circumferential stress



theory. The crack propagation simulations for Mode I case show acceptable crack path predictions even though simulated along with the geometry deformations. The results of the assessments strongly indicate that the finite element simulation for 2D linear elastic fracture mechanics problems has been successfully employed.

## References

- Andersen, M.R., 1998. Fatigue Crack Initiation and Growth in Ship Structures. Ph.D Thesis, Technical University of Denmark.
- Anderson, T.L., 1994. Fracture Mechanics: Fundamental and Applications (2nd Ed.). CRC Press.
- Ariffin, A.K., 1995. Powder Compaction, Finite Element Modelling and Experimental Validation. Ph.D Thesis, University of Wales Swansea.
- Bittencourt, T.N., Wawrzynek, P.A., Ingraffea, A.R., Sousa, J.L., 1996. Quasi-automatic simulation of crack propagation for 2D LEFM problems. *Engineering Fracture Mechanics*, **55**(2):321-334. [doi:10.1016/0013-7944(95)00247-2]
- Broek, D., 1986. Elementary Engineering Fracture Mechanics (4th Ed.). Martinus Nijhoff Publishers.
- de Matos, P.F.P., Moreira, P.M.G.P., Portela, A., de Castro, P.M.S.T., 2004. Dual boundary element analysis of cracked plates: post-processing implementation of the singularity subtraction technique. *Computers and Structures*, **82**(17-19):1443-1449. [doi:10.1016/j.compstruc.2004.03.040]
- El-Hamalawi, A., 2004. A 2D combined advancing front-delaunay mesh generation scheme. *Finite Elements in Analysis and Design*, **40**(9-10):967-989. [doi:10.1016/j.finel.2003.04.001]
- Fett, T., 1999. Stress intensity factors for edge-cracked plates under arbitrary loading. *Fatigue & Fracture of Engineering Materials & Structures*, **22**(4):301-305. [doi:10.1046/j.1460-2695.1999.00156.x]
- Freese, C.E., Baratta, F.I., 2006. Single edge-crack stress intensity factor solutions. *Engineering Fracture Mechanics*, **73**(5):616-625. [doi:10.1016/j.engfracmech.2005.09.003]
- Guinea, G.V., Planan, J., Elices, M., 2000.  $K_I$  evaluation by the displacement extrapolation technique. *Engineering Fracture Mechanics*, **66**(3):243-255. [doi:10.1016/S0013-7944(00)00016-3]
- Löhner, R., 1997. Automatic unstructured grid generators. *Finite Elements in Analysis and Design*, **25**(1-2):111-134. [doi:10.1016/S0168-874X(96)00038-8]
- Orange, T.W., 1988. Stress Intensity and Crack Displacement for Small Edge Cracks. NASA Technical Paper 2801.
- Parnas, L., Bilir, O.G., Tezcan, E., 1996. Strain gauge methods for measurement of opening mode stress intensity factor. *Engineering Fracture Mechanics*, **55**(3):485-492. [doi:10.1016/0013-7944(95)00214-6]
- Phongthanapanich, S., Dechaumphai, P., 2004. Adaptive delaunay triangulation with object-oriented programming for crack propagation analysis. *Finite Element in Analysis and Design*, **40**(13-14):1753-1771. [doi:10.1016/j.finel.2004.01.002]
- Portela, A., 1993. Dual Boundary Element Analysis of Crack Growth. Computational Mechanics Publications, Southampton, UK and Boston, USA.
- Sezer, L., Zeid, I., 1991. Automatic quadrilateral triangular free form mesh generation for planar region. *International Journal for Numerical Methods in Engineering*, **32**(7):1441-1483. [doi:10.1002/nme.1620320705]
- Simonsen, B.C., Tornqvist, R., 2004. Experimental and numerical modelling of ductile crack propagation in large-scale shell structures. *Marine Structures*, **17**(1):1-27. [doi:10.1016/j.marstruc.2004.03.004]
- Tada, H., Paris, P.C., Irwin, G.R., 2000. The Stress Analysis of Cracks Handbook. ASME Press, New York.
- Zhu, W.X., Smith, D.J., 1995. On the use of displacement extrapolation to obtain crack tip singular stresses and stress intensity factors. *Engineering Fracture Mechanics*, **51**(3):391-400. [doi:10.1016/0013-7944(94)00319-D]
- Zienkiewicz, O.C., Taylor, R.L., Zhu, J.Z., 2005. The Finite Element Method: Its Basis and Fundamentals (6th Ed.). Elsevier Butterworth-Heinemann.